ACS APPLIED MATERIALS & INTERFACES

Research Article

www.acsami.org

RTA-Treated Carbon Fiber/Copper Core/Shell Hybrid for Thermally Conductive Composites

Seunggun Yu,[†,‡] Bo-In Park,[†] Cheolmin Park,[‡] Soon Man Hong,[†] Tae Hee Han,[*,#] and Chong Min Koo[*,†,⊥]

[†]Center for Materials Architecturing, Korea Institute of Science and Technology, Seoul 136-791, Republic of Korea

[‡]Department of Materials Science and Engineering, Yonsei University, Seoul 120-749, Republic of Korea

[#]Department of Organic and Nano Engineering, Hanyang University, Seoul 133-791, Republic of Korea

[⊥]Nanomaterials Science and Engineering, University of Science and Technology, Daejeon 305-350, Republic of Korea

Supporting Information

ABSTRACT: In this paper, we demonstrate a facile route to produce epoxy/carbon fiber composites providing continuous heat conduction pathway of Cu with a high degree of crystal perfection via electroplating, followed by rapid thermal annealing (RTA) treatment and compression molding. Copper shells on carbon fibers were coated through electroplating method and post-treated via RTA technique to reduce the degree of imperfection in the Cu crystal. The epoxy/Cu-plated carbon fiber composites with Cu shell of 12.0 vol % prepared via simple compression molding, revealed 18 times larger thermal conductivity (47.2 W m^{-1} K^{-1}) in parallel direction and 6 times larger thermal conductivity (3.9 W m^{-1} K^{-1}) in perpendicular direction than epoxy/carbon fiber composite. Our novel composites with RTA-treated carbon fiber/Cu core/shell hybrid showed heat conduction behavior of an excellent polymeric composite thermal conductor with continuous heat conduction pathway, comparable to theoretical values obtained from Hatta and Taya model.

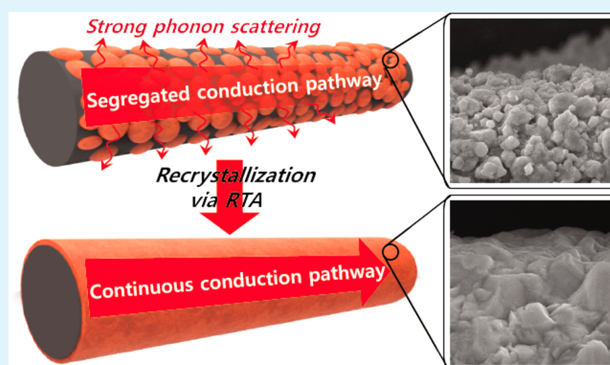

KEYWORDS: *thermal conductivity, composite, core/shell, rapid thermal annealing (RTA), carbon fiber, electroplating*

INTRODUCTION

Thermal management of polymeric composites has gained increasing interest as an efficient heat dissipation material, because it is directly related to the performance, lifetime, and reliability of a variety of devices, including LED, automobiles, aerospace systems, microelectronics, and photovoltaics.[1−3] The phonon energy, playing the main role in heat conduction, is transferred through vibration of elastic crystal structures.[4,5] However, common polymers have intrinsically low thermal conductivity (in the order of 0.1 W m^{-1} K^{-1}) due to some structural defects, such as low crystallinity and relatively low elastic modulus, causing strong phonon scattering.[6−8] Therefore, enhancement of thermal conductivities in polymeric composites has been achieved via the addition of thermally conductive fillers, including metallic,[9−12] inorganic,[13−17] and carbonaceous materials.[18−23]

To achieve effective heat conduction, the thermally conductive fillers need to be percolated in the composite materials. Unfortunately, the most particulate fillers established the continuous heat conduction pathway at very high filler contents of above 60−70 vol % in the composite.[24−26] The high filler content makes processing difficult and increases the cost.[27,28]

In this paper, we display a facile route to develop a continuous heat conduction pathway of Cu with a high degree of crystal perfection in the epoxy/carbon fiber (CF) composites via electroplating, rapid thermal annealing (RTA), and compression molding techniques. Continuous Cu conduction pathway was realized via Cu shell plating on the carbon fibers. The degree of perfection of Cu crystals on carbon fibers was improved through RTA treatment method. The electroplating has many advantages, such as simple processing under ordinary pressure—no need to make vacuum—and the ability to produce uniform coating on the non-flat surface materials.[29] However, the electroplating process accompanies hydrogen absorption, formation of bubbles, and incorporation of impurities from the plating solution on the plated layer.[30,31] These issues cause significant imperfection in the plated metal layer.[32,33] RTA treatment, using direct and strong radiation exposure from a halogen lamp in a short time, was introduced to enhance the crystal perfection of the coated Cu shell. The epoxy/carbon fiber composites with 12.0 vol % of RTA-treated

Received: February 11, 2014
Accepted: April 23, 2014
Published: April 23, 2014

ACS Publications © 2014 American Chemical Society

Cu shell, were prepared via simple compression molding process. The examined samples revealed the thermal conductivities of 47.2 W m^{-1} K^{-1} and 3.9 W m^{-1} K^{-1} in parallel and perpendicular directions, respectively. The thermal conductivity of the prepared composites linearly increased with the Cu content, even at very small contents. This observation was consistent with the theoretical values obtained from Hatta and Taya model. The heat conduction behavior of composites verifies that the novel architecture of Cu shells with the high crystallinity on the CF core is an excellent model system for heat conductive polymeric composites.

■ EXPERIMENTAL SECTION

Materials. Polyacrylonitrile (PAN)-based CFs with a diameter of 7.5 μm (CARBONEX, Hankuk Carbon Co., Ltd., Korea) were used as reinforcement. The thermal conductivities of carbon fiber were 8.04 and 0.84 W m^{-1} K^{-1} in parallel direction and perpendicular direction, respectively.[34] The epoxy resin was bisphenol A diglycidyl ether (YD-128, Kukdo Chemical Co., Ltd., Korea) with a molecular weight of 340.4 g mol^{-1} and an equivalent weight of 184 to 194 g eq^{-1}. As a curing agent, 4,4′-diaminodiphenylmethane (M0220, Tokyo Chemical Industry Co., Ltd., Japan) with a molecular weight of 198.3 g mol^{-1} and a reactive hydrogen equivalent weight of about 49.5 g eq^{-1} was used. This thermoset epoxy resin and the hardener were used as polymer matrix. Copper(II) sulfate pentahydrate and sulfuric acid (Daejung Chemicals, Korea) were used as received.

Preparation of Cu-Electroplated Carbon Fiber (Cu-p-CF). Cu was coated on the CF surfaces using an electroplating method that was conducted using a two-electrode system with CF cathode and Cu anode bar in the electrolyte. The electroplating solution consisted of 200 g L^{-1} copper(II) sulfate pentahydrate and 50 g L^{-1} sulfuric acid. Electroplating was performed at a current density of 0.70 A cm^{-2} and voltage of 0.50 V in a solution magnetically stirred at 300 rpm for 1, 2, 3, 4, or 5 h to achieve the desired Cu thickness as electroplating time was increasing. The fabricated Cu-p-CFs samples were rinsed with distilled water and then dried in vacuum for 2 h at 80 °C to prevent oxidation of the Cu layer of CF. For a typical sample, the number in the sample designation of the Cu-plated CF denotes the Cu-electroplating time, for instance Cu-p-CF_1 was electroplated for 1 h.

Preparation of Electroplated Cu Plate. The Cu was coated on the Al plate using an electroplating method with the conditions as CF electroplating. The electroplating was performed at a current density of 6.5 A cm^{-2} and voltage of 5.0 V in a solution magnetically stirred at 300 rpm for 24 h. The as-deposited Cu on the Al plate was rinsed and dried and then exfoliated from Al plate.

RTA Process of Cu-p-CF and Electroplated Cu. The recrystallization in both types of samples, including Cu-p-CF and electroplated Cu (as-deposited Cu), was performed through RTA process (RTP1003, SnTek Co., Korea). The samples were annealed at 300, 400, and 500 °C for 30 s in N_2 atmosphere. During the annealing process, the heating rate was kept at 40 °C s^{-1}.

Preparation of Epoxy/Cu-p-CF Composites. The fabrication procedure of Epoxy/Cu-p-CF composites is schematically shown in Figure 1. A moderate amount of bisphenol A diglycidyl ether was added to 4,4′-diaminodiphenylmethane at a weight ratio of 79:21 and blended using sonication at 300 W and 70 MHz for 1 h at 80 °C to obtain a homogeneous solution. Then, the mixture of epoxy resin and curing agent was poured on the Cu-p-CFs and the impregnated fibers were hot pressed and cured under pressure of 100 kPa for 30 min at 80 °C and then for 2 h at 150 °C.

Characterization Methods. The morphologies of Cu-p-CF and Epoxy/Cu-p-CF were examined using a scanning electron microscope with a field emission gun (SEM, FEI Inspect F50). The contents of Cu, CF, and epoxy were determined using thermogravimetric analysis (TGA, Q-50, TA Instruments) technique. The crystallographic properties of Cu-p-CF and Cu plate were investigated using X-ray diffraction (XRD, X'pert Pro. PANalytical) technique with Cu Kα radiation. Thermal diffusivity of the composites was measured with the laser flash method (LFA-447, Netzsch) at room temperature. Specific heats of samples were examined with differential scanning calorimetry (DSC, Q-20, TA Instruments). Thermal conductivity was calculated according to ASTM E 1461-92 using the equation $k = T_d \rho C_p$, where k, T_d, ρ, and C_p are the thermal conductivity (W m^{-1} K^{-1}), thermal diffusivity (mm^2 s^{-1}), density (g cm^{-3}), and specific heat capacity (J g^{-1} K^{-1}), respectively.

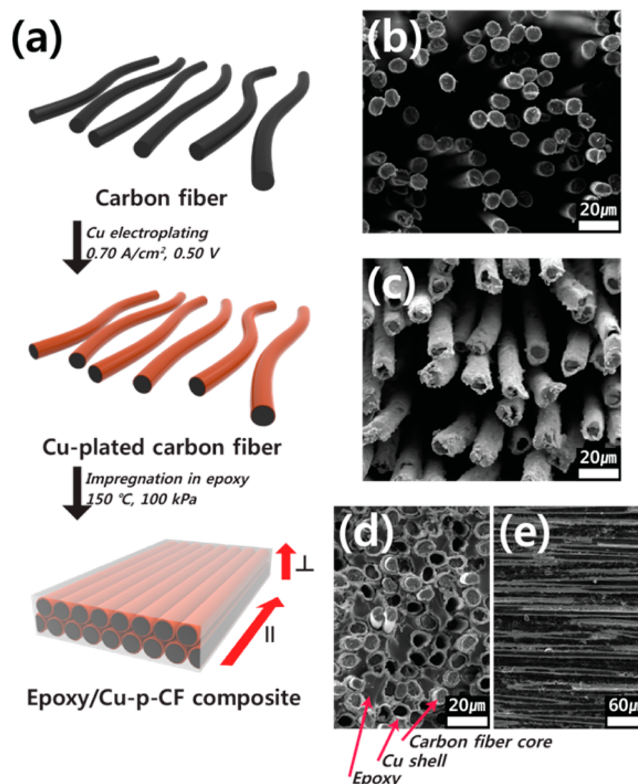

Figure 1. (a) Schematic of fabrication process of epoxy/Cu-p-CF composite and cross-view SEM micrographs of (b) pristine CF, (c) Cu-p-CF, (d) epoxy/Cu-p-CF composite and side-view SEM micrograph (e) epoxy/Cu-p-CF composite. Arrows in part d indicate the epoxy matrix, Cu shell, and carbon fiber core.

■ RESULTS AND DISCUSSION

Figure 1a shows a schematic of the fabrication process of Epoxy/Cu-p-CF composite. The Cu layer was uniformly coated on the surface of CFs using an electroplating method in which the Cu shell on the CF was deposited (Figure 1b,c). As shown in Supporting Information Figure S1, the thickness of the Cu shell on CF was easily controlled with electroplating time. We denoted the prepared Cu-plated CF samples as Cu-p-CF_1 (1 h), Cu-p-CF_2 (2 h), and so on, according to the electroplating time. The Cu-p-CF hybrids were impregnated with epoxy resin and molded to prepare composites under high pressures with a well-packed state (Figure 1d,e). The contents of epoxy, CF, and Cu in the epoxy/CF and epoxy/Cu-p-CF composites, determined using TGA technique (Supporting Information Figure S2), are listed in Table 1 and were directly converted into the thickness of Cu shells.

Figure 2 shows the X-ray diffraction patterns of Cu-p-CFs prepared at various electroplating time. As-electroplated Cu XRD patterns reveal the three major characteristic reflection peaks of (111), (200), and (220), indicating a typical face-centered cubic (FCC) crystal structure for Cu layer.[35] In Cu-p-CF_1 sample, the peak intensity of (220) reflection is larger

Table 1. Characterization of Epoxy/Cu-p-CF Composites before and after the RTA Process

sample name	volume (%)[a] Cu	CF	epoxy	density (g cm^{-3})	specific heat (J g^{-1} K^{-1})	thermal diffusivity (mm^2 s^{-1}) before RTA $T_{d\parallel}$	before RTA $T_{d\perp}$	after RTA $T_{d\parallel}$	after RTA $T_{d\perp}$	thermal conductivity (W m^{-1} K^{-1}) before RTA $k_{\parallel}$	before RTA $k_{\perp}$	after RTA $k_{\parallel}$	after RTA $k_{\perp}$
epoxy/CF	0	48.5	51.5	1.4	1.03	1.8	0.4			2.6	0.7		
epoxy/Cu-p-CF_1	5.2	33.8	61.0	1.7	1.05	4.1	0.3	9.2	0.8	7.5	0.6	16.8	0.8
epoxy/Cu-p-CF_2	7.6	26.3	66.1	1.8	0.98	5.6	0.9	16.0	1.9	10.2	1.7	28.9	1.9
epoxy/Cu-p-CF_3	10.4	18.0	71.6	2.6	1.00	9.5	0.8	14.5	2.7	24.4	2.1	36.2	2.7
epoxy/Cu-p-CF_4	11.4	16.0	72.6	2.8	0.95	12.7	1.3	17.0	3.6	34.2	3.4	45.7	3.6
epoxy/Cu-p-CF_5	12.0	14.2	73.8	3.0	0.97	12.1	1.2	16.1	3.9	35.4	3.5	47.2	3.9

[a]Estimated with thermogravimetric analysis.

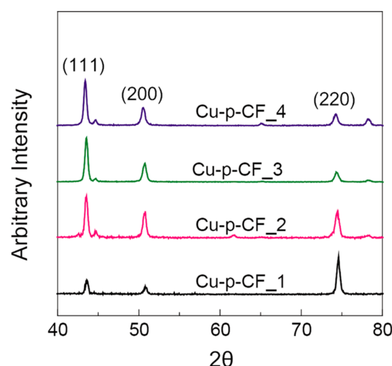

Figure 2. XRD patterns of Cu-p-CF with electroplating time.

than those of (111) and (200) reflections. As the electroplating time increased, the peak intensity of (111) gradually increased and surpassed the intensities of the other two peaks. This observation is due to the directional growth nature of Cu layer during electroplating process.[36] Firstly, as-deposited Cu mainly grows along (220) direction on CF substrate in the initial step of electroplating process. After that, Cu grows along (111) direction on Cu layer because the Cu prefers orientation of (111) with the least energy. Copper grown via electroplating method has high degree of polycrystallinity, small grain size, and high porosity due to its imperfection.[30]

The RTA process was introduced to reduce the degree of imperfection of as-deposited Cu layer. The epoxy/Cu-p-CF composites with as-deposited Cu shell layer showed irregular morphology and the surface of composites were getting rougher with increasing the electroplating time as shown in Supporting Information Figure S3. The as-deposited Cu layer in the Cu-p-CF_5 sample revealed intensely rough surface with granular shaped morphology as shown in Figure 3a,b. After RTA process, the Cu domains were fused each other, and the surface texture of the Cu layer became smooth without pores, and the domain size was increased as shown in Figure 3c,d and Supporting Information Figure S4. The RTA treatment induced the preferential directional grain growth to the (111) direction during the recrystallization of Cu crystals (Supporting Information Figure S5). From the XRD results, the average crystallite size (D_p) of electroplated Cu layer was calculated using the Scherrer equation as follows[37]

$$D_p = \frac{0.94\lambda}{\beta \cos \theta} \tag{1}$$

where D_p is average crystallite size, λ is wavelength of X-ray, β is line full width at half maximum (FWHM) intensity in

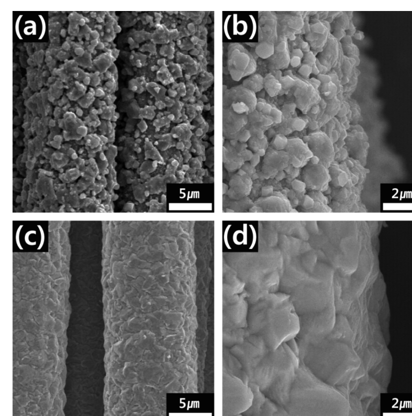

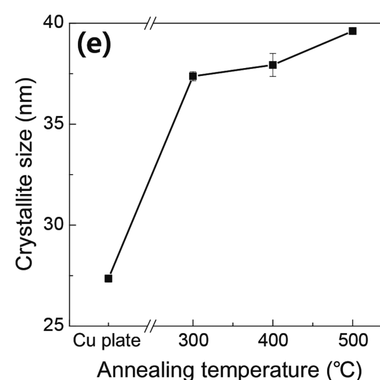

Figure 3. SEM images of surfaces of (a,b) as-deposited Cu layer for 5 h, (c,d) RTA treated Cu layer at 500 °C in different magnifications. (e) Plots of crystallite size from the (111) reflection peak of Cu-p-CF.

diffraction profile, and θ is Bragg angle. The crystallite size of Cu layer increased with annealing temperature (Figure 3e). The crystallite size of as-deposited Cu layer was 27 nm in the (111) preferred orientation, while that of RTA-treated sample (500 °C) increased up to 40 nm.

Figure 4a shows the thermal conductivities of epoxy/Cu-p-CF composites in the parallel direction. The epoxy/CF composite revealed a thermal conductivity value of 2.6 W m^{-1} K^{-1}. The thermal conductivities of epoxy/Cu-p-CF composites increased with Cu content regardless of RTA treatment. Before the RTA process, the epoxy/Cu-p-CF_5 sample with the Cu content of 12.0 vol % (thickness 1.1 μm) exhibited nearly 14 times larger thermal conductivity (35.4 W m^{-1} K^{-1}) than the epoxy/CF composite. After the RTA process, the thermal conductivity of the epoxy/Cu-p-CF_5

dx.doi.org/10.1021/am500871b | ACS Appl. Mater. Interfaces 2014, 6, 7498−7503

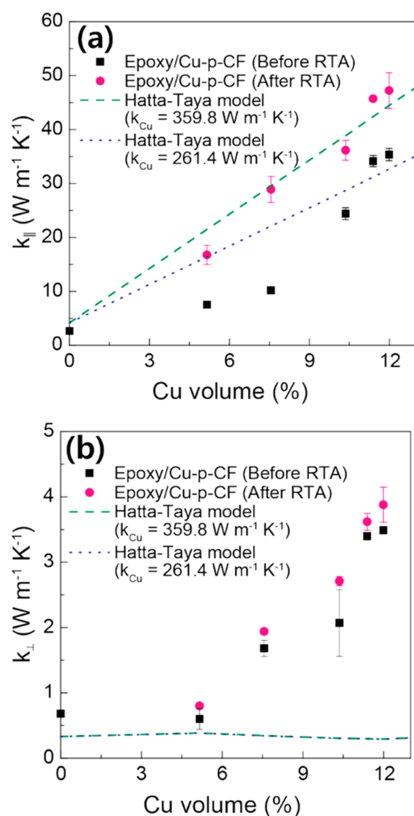

Figure 4. (a) $k_{\parallel}$ and (b) $k_{\perp}$ of epoxy/Cu-p-CF composites in parallel and perpendicular directions, respectively. The green dashed and blue dotted lines represent the theoretical thermal conductivities of epoxy/Cu-p-CF composites calculated using Hatta and Taya equations with considerations of k_{Cu} = 359.8 and k_{Cu} = 261.4 W m^{-1} K^{-1}, as thermal conductivities of RTA-treated Cu layers at 500 °C and of as-electroplated Cu layers, respectively.

sample revealed nearly 18 times larger thermal conductivity (47.2 W m^{-1} K^{-1}) by enlarged grain and domain size.[38]

Figure 4b shows the thermal conductivities of epoxy/Cu-p-CF composites in the perpendicular direction. The epoxy/CF composite revealed a thermal conductivity value of 0.7 W m^{-1} K^{-1} in this direction. The thermal conductivities of epoxy/Cu-p-CF composites also increased with Cu content regardless of RTA treatment. Before the RTA process, the epoxy/Cu-p-CF_5 sample with a Cu content of 12.0 vol % exhibited nearly 5 times larger thermal conductivity (3.5 W m^{-1} K^{-1}) than the epoxy/CF composite. After the RTA process, the thermal conductivity of the epoxy/Cu-p-CF_5 composite revealed nearly 6 times larger thermal conductivity (3.9 W m^{-1} K^{-1}).

The experimental results of epoxy/Cu-p-CF composites were compared with the theoretical calculations using Hatta and Taya model.[39] The model assumes that fibers are unidirectionally aligned and uniformly packed in the composite, as illustrated in Figure 1a. When the fibers are oriented parallel to the direction of thermal conduction, the thermal conductivity of the composites in parallel direction ($k_{\parallel}$) is simply expressed by following equation

$$k_{\parallel} = (V_f k_f) + (V_m k_m) \tag{2}$$

where $k_{\parallel}$ is the thermal conductivity of the composite in the parallel direction of fibers, V_f is the volume fraction of the fiber, k_f is the thermal conductivity of the fiber, V_m is the volume fraction of the matrix, and k_m is the thermal conductivity of matrix. The k_f values of the Cu-p-CF were calculated in the same manner

$$k_f = (V_{Cu} k_{Cu}) + (V_{CF} k_{CF}) \tag{3}$$

where V_{Cu} and V_{CF} are the volume fractions of Cu and CF, respectively and k_{Cu} and k_{CF} are the thermal conductivities of Cu and CF, respectively.

When the fibers are oriented perpendicular to the direction of thermal conduction, the thermal conductivity of composites in perpendicular direction ($k_{\perp}$) is expressed by this equation

$$k_{\perp} = k_m + \frac{\{k_m(k_f - k_m)V_f\}}{\left\{k_m + V_m(k_f - k_m)\frac{1}{2}\right\}} \tag{4}$$

The calculated $k_{\parallel}$ and $k_{\perp}$ values were plotted as green-dashed and blue-dotted lines in Figure 4a,b. The green dashed and blue dotted lines were obtained from Hatta and Taya model with consideration of k_{Cu} = 359.8 and 261.4 W m^{-1} K^{-1}, respectively for RTA-treated Cu layers at 500 °C and for as-electroplated Cu layers, as shown in Supporting Information Figure S6.

The calculated $k_{\parallel}$ of epoxy/Cu-p-CF composites agreed well with the measured $k_{\parallel}$. Especially, thermal conductivity of the epoxy/RTA-treated Cu-p-CF composites satisfied the clear linear relationship with the Cu content, indicating that Cu shell worked as a continuous heat conduction pathway in the composites even at very low contents. In contrast, the calculated $k_{\perp}$ of epoxy/Cu-p-CF composites was quite different from the measured $k_{\perp}$ values. Theory could not predict the thermal conductivity of composites containing Cu in the perpendicular direction. The discrepancy is from the difference between theory and reality. The model assumes each fiber in the composite as a separate body in the perpendicular direction. However, in reality long fibers are likely to bump into each other. Contacts between adjacent Cu-p-CFs increase the thermal conductivity of the composites because heat conduction through the contacted fibers is much more favorable than that between the separate fibers insulated by epoxy matrix.

■ CONCLUSIONS

We demonstrated a versatile route to develop a continuous heat conduction pathway of Cu with a high degree of crystal perfection in the epoxy/CF composites via electroplating, RTA, and compression molding techniques. Carbon fibers played as an effective template for the formation of continuous Cu heat conduction pathway. The RTA treatment helped the electroplated Cu crystals to recrystallize, as a result, reducing the degree of crystal imperfection and increasing crystal size. The epoxy/carbon fiber composites made of 12.0 vol % RTA-treated Cu shell revealed the thermal conductivity of 18 times larger in parallel direction (47.2 W m^{-1} K^{-1}) and 6 times larger in perpendicular direction (3.9 W m^{-1} K^{-1}) than that of epoxy/carbon fiber composite. The thermal conductivity of epoxy/RTA-treated Cu-p-CF composite linearly increases with the Cu content even at very small amounts, which agrees well with the theoretical values obtained from Hatta and Taya model. The heat conduction behavior verifies that the novel architecture of core-shell hybrid of conductive Cu shells with the high crystallinity is an excellent system for heat conductive polymeric composites with continuous heat conduction pathway.

■ ASSOCIATED CONTENT

Supporting Information

Thickness of electroplated Cu shell on CF, TGA curves, SEM images of Cu-p-CFs, XRD reflection peaks, and thermal conductivities of Cu plates. This material is available free of charge via the Internet at http://pubs.acs.org/.

■ AUTHOR INFORMATION

Corresponding Authors

*Tel.: +82-2-958-6872. Fax: +82-2-958-5309. E-mail: koo@kist.re.kr.

*Email: than@hanyang.ac.kr.

Notes

The authors declare no competing financial interest.

■ ACKNOWLEDGMENTS

This work was supported by a grant from the Fundamental R&D Program for Technology of World Premier Materials funded by the Ministry of Knowledge Economy (MKE) and was partially supported by the Institute for Multi-disciplinary Convergence of Materials (IMCM) of the Korea Institute of Science and Technology (KIST) and the research fund of Hanyang University (HY-2013).

■ ABBREVIATIONS

CF, carbon fiber
RTA, rapid thermal annealing
Cu-p-CF, Cu-plated carbon fiber
PAN, polyacrylonitrile
SEM, scanning electron microscope
TGA, thermogravimetric analysis
XRD, X-ray diffraction
DSC, differential scanning calorimetry
FCC, face-centered cubic

■ REFERENCES

(1) Balandin, A. A. Thermal Properties of Graphene and Nanostructured Carbon Materials. *Nat. Mater.* **2011**, *10*, 569−581.

(2) Liang, Q.; Yao, X.; Wang, W.; Liu, Y.; Wong, C. P. A Three-Dimensional Vertically Aligned Functionalized Multilayer Graphene Architecture: An Approach for Graphene-Based Thermal Interfacial Materials. *ACS Nano* **2011**, *5*, 2392−2401.

(3) Marconnet, A. M.; Yamamoto, N.; Panzer, M. A.; Wardle, B. L.; Goodson, K. E. Thermal Conduction in Aligned Carbon Nanotube−Polymer Nanocomposites with High Packing Density. *ACS Nano* **2011**, *5*, 4818−4825.

(4) Zaitlin, M. P.; Anderson, A. C. Phonon Thermal Transport in Noncrystalline Materials. *Phys. Rev. B* **1975**, *12*, 4475−4486.

(5) Jagannathan, A.; Orbach, R.; Entin-Wohlman, O. Thermal Conductivity of Amorphous Materials above the Plateau. *Phys. Rev. B* **1989**, *39*, 13465−13477.

(6) Yorifuji, D.; Ando, S. Molecular Structure Dependence of Out-of-Plane Thermal Diffusivities in Polyimide Films: A Key Parameter for Estimating Thermal Conductivity of Polymers. *Macromolecules* **2010**, *43*, 7583−7593.

(7) Shen, S.; Henry, A.; Tong, J.; Zheng, R.; Chen, G. Polyethylene Nanofibers with Very High Thermal Conductivities. *Nat. Nanotechnol.* **2010**, *5*, 251−255.

(8) Choy, C. L. Thermal Conductivity of Polymers. *Polymer* **1977**, *18*, 984−1004.

(9) Mamunya, Y. P.; Davydenko, V. V.; Pissis, P.; Lebedev, E. V. Electrical and Thermal Conductivity of Polymers Filled with Metal Powders. *Eur. Polym. J.* **2002**, *38*, 1887−1897.

(10) Yu, S.; Lee, J.-W.; Han, T. H.; Park, C.; Kwon, Y.; Hong, S. M.; Koo, C. M. Copper Shell Networks in Polymer Composites for Efficient Thermal Conduction. *ACS Appl. Mater. Interfaces* **2013**, *5*, 11618−11622.

(11) Pashayi, K.; Fard, H. R.; Lai, F.; Iruvanti, S.; Plawsky, J.; Borca-Tasciuc, T. High Thermal Conductivity Epoxy-Silver Composites Based on Self-Constructed Nanostructured Metallic Networks. *J. Appl. Phys.* **2012**, *111*, 104310.

(12) Yorifuji, D.; Ando, S. Enhanced Thermal Diffusivity by Vertical Double Percolation Structures in Polyimide Blend Films Containing Silver Nanoparticles. *Macromol. Chem. Phys.* **2010**, *211*, 2118−2124.

(13) Terao, T.; Zhi, C.; Bando, Y.; Mitome, M.; Tang, C.; Golberg, D. Alignment of Boron Nitride Nanotubes in Polymeric Composite Films for Thermal Conductivity Improvement. *J. Phys. Chem. C* **2010**, *114*, 4340−4344.

(14) Tanimoto, M.; Yamagata, T.; Miyata, K.; Ando, S. Anisotropic Thermal Diffusivity of Hexagonal Boron Nitride-Filled Polyimide Films: Effects of Filler Particle Size, Aggregation, Orientation, and Polymer Chain Rigidity. *ACS Appl. Mater. Interfaces* **2013**, *5*, 4374−4382.

(15) Li, T.-L.; Hsu, S. L.-C. Enhanced Thermal Conductivity of Polyimide Films via a Hybrid of Micro- and Nano-Sized Boron Nitride. *J. Phys. Chem. B* **2010**, *114*, 6825−6829.

(16) Sato, K.; Horibe, H.; Shirai, T.; Hotta, Y.; Nakano, H.; Nagai, H.; Mitsuishi, K.; Watari, K. Thermally Conductive Composite Films of Hexagonal Boron Nitride and Polyimide with Affinity-Enhanced Interfaces. *J. Mater. Chem.* **2010**, *20*, 2749−2752.

(17) Terao, T.; Bando, Y.; Mitome, M.; Zhi, C.; Tang, C.; Golberg, D. Thermal Conductivity Improvement of Polymer Films by Catechin-Modified Boron Nitride Nanotubes. *J. Phys. Chem. C* **2009**, *113*, 13605−13609.

(18) Song, S. H.; Park, K. H.; Kim, B. H.; Choi, Y. W.; Jun, G. H.; Lee, D. J.; Kong, B.-S.; Paik, K.-W.; Jeon, S. Enhanced Thermal Conductivity of Epoxy-Graphene Composites by Using Non-Oxidized Graphene Flakes with Non-Covalent Functionalization. *Adv. Mater.* **2013**, *25*, 732−737.

(19) Yu, A.; Ramesh, P.; Sun, X.; Bekyarova, E.; Itkis, M. E.; Haddon, R. C. Enhanced Thermal Conductivity in a Hybrid Graphite Nanoplatelet—Carbon Nanotube Filler for Epoxy Composites. *Adv. Mater.* **2008**, *20*, 4740−4744.

(20) Potts, J. R.; Shankar, O.; Du, L.; Ruoff, R. S. Processing Morphology−Property Relationships and Composite Theory Analysis of Reduced Graphene Oxide/Natural Rubber Nanocomposites. *Macromolecules* **2012**, *45*, 6045−6055.

(21) Tang, Z.; Kang, H.; Shen, Z.; Guo, B.; Zhang, L.; Jia, D. Grafting of Polyester onto Graphene for Electrically and Thermally Conductive Composites. *Macromolecules* **2012**, *45*, 3444−3451.

(22) Balandin, A. A.; Ghosh, S.; Bao, W.; Calizo, I.; Teweldebrhan, D.; Miao, F.; Lau, C. N. Superior Thermal Conductivity of Single-Layer Graphene. *Nano Lett.* **2008**, *8*, 902−907.

(23) Shahil, K. M. F.; Balandin, A. A. Graphene-Multilayer Graphene Nanocomposites as Highly Efficient Thermal Interface Materials. *Nano Lett.* **2012**, *12*, 861−867.

(24) Ishida, H.; Rimdusit, S. Very High Thermal Conductivity Obtained by Boron Nitride-Filled Polybenzoxazine. *Thermochim. Acta* **1998**, *320*, 177−186.

(25) Lee, E.-S.; Lee, S.-M.; Shanefield, D. J.; Cannon, W. R. Enhanced Thermal Conductivity of Polymer Matrix Composite via High Solids Loading of Aluminum Nitride in Epoxy Resin. *J. Am. Ceram. Soc.* **2008**, *91*, 1169−1174.

(26) Qian, R.; Yu, J.; Wu, C.; Zhai, S.; Jiang, P. Alumina-Coated Graphene Sheet Hybrids for Electrically Insulating Polymer Composites with High Thermal Conductivity. *RSC Adv.* **2013**, *3*, 17373−17379.

(27) Yoshihara, S.; Ezaki, T.; Nakamura, M.; Watanabe, J.; Matsumoto, K. Enhanced Thermal Conductivity of Thermoplastics by Lamellar Crystal Alignment of Polymer Matrices. *Macromol. Chem. Phys.* **2010**, *211*, 2118−2124.

(28) Yu, S.; Kim, D.-K.; Park, C.; Hong, S. M.; Koo, C. M. Thermal Conductivity Behavior of SiC-Nylon 6,6 and hBN-Nylon 6,6 Composites. *Res. Chem. Intermed.* **2014**, *40*, 33−40.
(29) Gabe. D. R. *Principles of Metal Surface Treatment and Proptection*; Pergamon Press: Oxford, 1978.
(30) Stangl, M.; Acker, J.; Oswald, S.; Uhlemann, M.; Gemming, T.; Baunack, S.; Wetzig, K. Incorporation of Sulfur, Chlorine, and Carbon into Electroplated Cu Thin Films. *Microelectron. Eng.* **2007**, *84*, 54−59.
(31) Chang, S.-C.; Shieh, J.-M.; Dai, B.-T.; Feng, M.-S. Reduction of Resistivity of Electroplated Copper by Rapid Thermal Annealing. *Electrochem. Solid-State Lett.* **2002**, *5*, C67−C70.
(32) Strehle, S.; Bartha, J. W.; Wetzig, K. Electrical Properties of Electroplated Cu(Ag) Thin Films. *Thin Solid Films* **2009**, *517*, 3320−3325.
(33) Seah, C. H.; Mridha, S.; Chan, L. H. Annealing of Copper Electrodeposits. *J. Vac. Sci. Technol., A* **1999**, *17*, 1963−1967.
(34) Goo, N. S.; Moon, Y. K.; Woo, K. Effective Thermal Conductivities of CF3327 Plain-Weave Fabric Composite. *Compos. Res.* **2002**, *15*, 27−34.
(35) Glocker, R.; Kaupp, E. Über die Faserstruktur elektrolytischer Metallniederschläge. *Z. Phys. A* **1924**, *24*, 121−139.
(36) Lin, C.-T.; Lin, K.-L. Effects of Current Density and Deposition Time on Electrical Resistivity of Electroplated Cu Layers. *J. Mater. Sci.: Mater. Electron.* **2004**, *15*, 757−762.
(37) Scherrer, P. Estimation of the Size and Internal Structure of Colloidal Particles by Means of Röntgen Rays. *Gött. Nachr.* **1918**, *2*, 98−100.
(38) Feng, B.; Li, Z.; Zhang, X. Prediction of Size Effect on Thermal Conductivity of Nanoscale Metallic Films. *Thin Solid Films* **2009**, *517*, 2803−2807.
(39) Hiroshi, H.; Minoru, T. Equivalent Inclusion Method for Steady State Heat Conduction in Composites. *Int. J. Eng. Sci.* **1986**, *24*, 1159−1172.